

# Desorption of ionic species from ice/graphite by femtosecond XUV free-electron laser pulses

B Siemer<sup>1</sup>, T Hoger<sup>1</sup>, M Rutkowski<sup>1</sup>, R Treusch<sup>2</sup> and H Zacharias<sup>1</sup>

<sup>1</sup> Physikalisches Institut, Westfälische Wilhelms-Universität Münster, Wilhelm Klemm Strasse 10, 48149 Münster, Germany

<sup>2</sup> HASYLAB, Deutsches Elektronen-Synchrotron DESY, Notkestrasse 85, 22607 Hamburg, Germany

E-mail: [B.Siemer@uni-muenster.de](mailto:B.Siemer@uni-muenster.de)

Received 24 August 2009, in final form 17 September 2009

Published 4 February 2010

Online at [stacks.iop.org/JPhysCM/22/084013](http://stacks.iop.org/JPhysCM/22/084013)

## Abstract

We report results of laser desorption from water ice surfaces using XUV pulses from the free-electron laser in Hamburg (FLASH). This XUV to soft x-ray FEL provides femtosecond pulses at 20–200 eV photon energy with pulse energies up to 100  $\mu$ J. The interaction of this intense soft x-ray radiation with ice ( $\text{H}_2\text{O}$ ,  $\text{D}_2\text{O}$ ) adsorbed on highly oriented pyrolytic graphite (HOPG) yields the desorption of various ions, particularly  $\text{H}^+$  ( $\text{D}^+$ ),  $\text{O}^+$ ,  $\text{O}_2^+$  and others. For  $\text{H}^+$  and  $\text{O}^+$  ions linear desorption yields are observed, while for  $\text{O}_2^+$  a highly nonlinear desorption yield with  $n = (2.5 \pm 0.2)$  is found. Kinetic energies of 1.8 eV, 559 meV and 390 meV for  $\text{H}^+$ ,  $\text{O}^+$ , and  $\text{O}_2^+$ , respectively, account for only a small part of the available excess energy.

(Some figures in this article are in colour only in the electronic version)

## 1. Introduction

The photodesorption of water from icy grains in the interstellar medium and in circumstellar discs is considered to be a major source for gas phase  $\text{H}_2\text{O}$  in such clouds. Also in the upper atmosphere this process might have an influence on the reaction kinetics. Despite the expected implications on the microscopic and macroscopic behaviour of cosmic clouds only a few studies at high photon energies have been devoted to investigating this process. In one of the first investigations Madey and co-workers studied the kinetic energy release into  $\text{H}^+$  desorbing from  $\text{H}_2\text{O}$  adsorbed on Ti and  $\text{TiO}_2$  surfaces [1, 2]. Near the threshold production from ice, at about 20 to 21 eV, which is considerably higher than in the gas phase, slow  $\text{H}^+$  ions are found [3], while at higher photon energies fast ions are observed. Chakarov and Kasemo investigated photoinduced processes in water ice on graphite at photon energies below 6 eV, where the co-adsorption of alkalis promote and facilitate desorption and dissociation [4–6]. Westley *et al* [7] studied the desorption yield of neutral  $\text{H}_2\text{O}$  from thick ice layers at the Lyman- $\alpha$

wavelength and obtained a yield of about  $5 \times 10^{-3}$ /photon. In addition various dissociation and photochemical reaction products have been observed, such as OH,  $\text{H}_2\text{O}_2$  and  $\text{HO}_2$  using Lyman- $\alpha$  and UV photons [8, 9]. Notably molecular [10] and atomic [9] hydrogen has been observed by irradiation with vacuum ultraviolet excimer laser radiation. Recently, in an extensive investigation Öberg *et al* [11] determined the temperature dependence of the desorption yield of water and neutral products by applying broadband VUV radiation (120–170 nm) from a hydrogen discharge lamp. Baggott *et al* studied the desorption of positive ions after irradiating the ice surfaces on graphite by continuous He I ( $h\nu = 21.2$  eV) and He II ( $h\nu = 40.8$  eV) lamp radiation [12]. At the higher photon energy, reactively formed product ions were observed which were absent at the lower photon energy. In this paper we report the first results on the direct desorption of ions from amorphous ice after irradiation with femtosecond XUV pulses provided by the free-electron laser at Hamburg by FLASH at DESY. The photon energies chosen are close to and above the He II resonance lines. Besides the relative yield of the parent and fragment ions, the kinetic energy release for  $\text{H}^+$ ,  $\text{O}^+$ , and  $\text{O}_2^+$  is

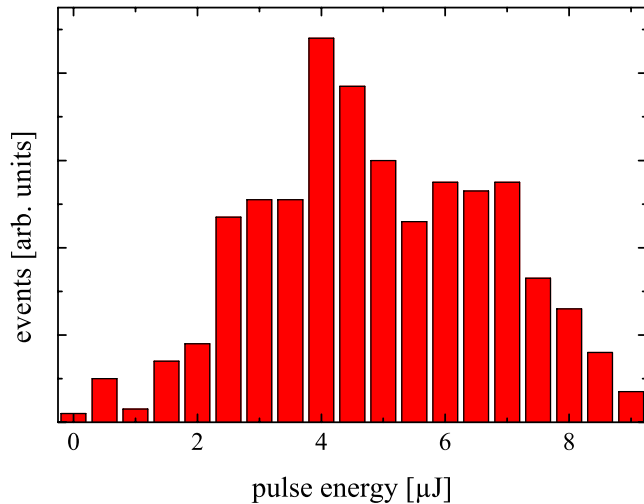


**Figure 1.** Distribution of FEL pulse energies at 58 eV for the desorption measurement; 500 pulses are shown.

determined. We trace the desorption to an electronic transition in the ice, and due to the high intensity multiple excitation processes may also be involved.

## 2. Experiment

The experiment is performed in beamline 1 at FLASH. In this beamline the XUV beam is weakly focused and strikes the analysed surface at an angle of incidence of  $67.5^\circ$  relative to the surface normal under the  $\hat{p}$ -polarization. Due to the oblique incidence a  $200 \times 300 \mu\text{m}^2$  ellipsoidal spot with an area of  $0.19 \text{ mm}^2$  is produced on the graphite sample. FLASH is operated at a photon energy of  $h\nu = 38$  and  $58 \text{ eV}$  in a  $5 \text{ Hz}$  single bunch mode with a spectral energy width of about  $0.8 \text{ eV}$ . Figure 1 shows the typical distribution of the energies of the FEL pulses during a desorption run at  $58 \text{ eV}$ . An averaged pulse energy of  $4.8 \pm 0.2 \mu\text{J}$  resulting in a fluence of  $2.55 \pm 0.1 \text{ mJ cm}^{-2}$  is applied to the ice surfaces. The pulse duration is about  $30 \text{ fs}$  [13].

A highly oriented pyrolytic graphite (HOPG) crystal of  $10 \text{ mm}$  diameter and with a mosaic angle of  $0.4^\circ$  serves as the sample. It is mounted on a liquid nitrogen containing reservoir attached to a holder on an  $X$ - $Y$ - $Z$  stage in an ultra-high vacuum chamber. The UHV chamber is evacuated by an oil free pump system to a base pressure of  $7 \times 10^{-10} \text{ Torr}$ . The HOPG crystal is prepared by cleaving with adhesive tape and annealing to  $800 \text{ K}$  by electron bombardment from the rear side. After sample preparation the temperature of the graphite crystal is held at  $95 \text{ K}$ , as monitored with a  $k$ -type thermocouple attached to the surface.  $\text{H}_2\text{O}$  and  $\text{D}_2\text{O}$  is dosed to the surface at normal incidence for several minutes at  $95 \text{ K}$  through a capillary with a constant pressure. Two coverages of  $30 \text{ ML}$  at  $58 \text{ eV}$  and  $80 \text{ ML}$  at  $38 \text{ eV}$  are prepared and investigated. At this temperature the sticking coefficient is assumed to be unity [14, 15]. At temperatures below  $100 \text{ K}$  water condenses as microporous amorphous ice [16, 17]. At the XUV photon energies employed the penetration depth into ice amounts to about  $5 \text{ nm}$  and  $15.7 \text{ nm}$  for  $38 \text{ eV}$  and  $58 \text{ eV}$

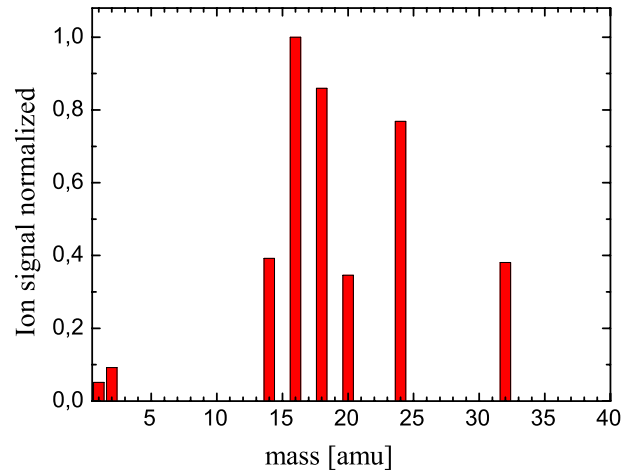


**Figure 2.** Masses observed after illuminating the  $\text{D}_2\text{O}$  ice surface with  $58 \text{ eV}$ . The ion yields are normalized to the  $\text{O}^+$  signal.

radiation, respectively [18, 19]. At an incident angle of  $\theta = 67.5^\circ$  only the top most 6 and 18 ML are irradiated with a monolayer (ML) water definition of  $1.15 \times 10^{15} \text{ molecules cm}^{-2}$ . It should be noted that at these photon energies and incidence angle about 12% and 5%, respectively, of the incident radiation is reflected.

Desorbing cations are measured by a Wiley–McLaren type time-of-flight mass spectrometer (TOF) mounted along the surface normal direction. Thereby the sample serves as the first repelling electrode. The output of the micro channel plates is directly monitored on a digital oscilloscope, gated and forwarded to a computer. The time-of-flight mass spectra are summed over 500 single shots. For each shot the signal and the FEL pulse energy are stored. Normalization and averaging occurred in the data analysis. Operating the TOF at low voltages allows us to derive the velocity of the ions from the broadening of the peaks by simulating their trajectories with SIMION.

## 3. Results and discussion

### 3.1. Mass spectra

After illuminating the ice-covered graphite surface with XUV radiation, different ions are directly detected by the time-of-flight mass spectrometer. It should be noted that the  $\text{H}_2\text{O}$  ice surfaces were illuminated with photon energies of  $38 \text{ eV}$  and the  $\text{D}_2\text{O}$  ice-covered surfaces with radiation of  $58 \text{ eV}$ . Both experiments show the expected monomer ion  $\text{H}_2\text{O}^+$  ( $\text{D}_2\text{O}^+$ ), dissociative fragments  $\text{H}^+$  ( $\text{D}^+$ ),  $\text{OH}^+$  ( $\text{OD}^+$ ), and  $\text{O}^+$ . Figure 2 shows a typical stick diagram for direct ion desorption from a  $\text{D}_2\text{O}$  ice surface. In addition to the fragment ions mentioned in both cases reactively formed  $\text{O}_2^+$  ions are also detected, however,  $\text{D}_3\text{O}^+$  ions are not observed which would be expected from the ionization of isolated water clusters on the surface.

The surprising appearance of signals at  $14$  and  $24 \text{ amu}$  ( $\text{CD}^+$  and  $\text{C}_2^+$ ) are only observed for the thin (nominally about  $30 \text{ ML}$ )  $\text{D}_2\text{O}$  layer at the high photon energy. At this photon

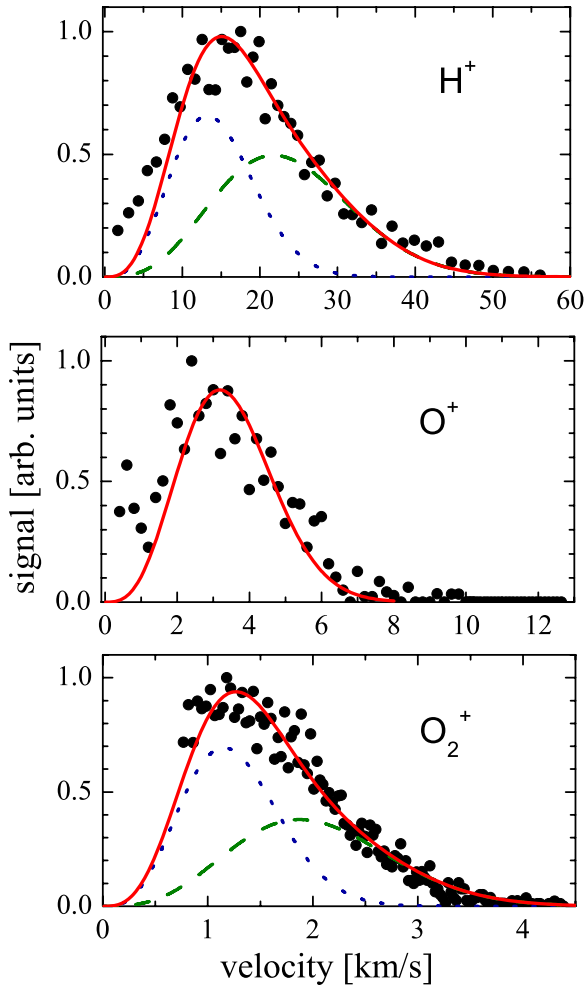


**Figure 3.** Velocity distribution of the desorbing ions. The black dots represent the measured data, while the solid line shows the fitted Maxwellian flux distributions. Thereby the dashed and dotted lines are for different temperatures. The Maxwellian distributions yield average energies of 1.8 eV, 840 meV and 390 meV for  $\text{H}^+$ ,  $\text{O}^+$  and  $\text{O}_2^+$  ions, respectively.

energy the  $1/e$  penetration amounts to about 18 ML, thus for nominally 30 ML thin layers a finite amount of radiation is able to reach the HOPG surface. In addition, due to the mosaic structure the HOPG step edges might show a lower coverage and in addition may provide some field enhancement for the XUV radiation. At present, however, a satisfying explanation has to await further beamtime.

The most dominant ions are  $\text{O}^+$  and  $\text{OD}^+$ . These observations deviate significantly from the findings of Baggott *et al* using a continuous light source at  $h\nu = 40.8$  eV [12]. There,  $\text{D}_3\text{O}^+$  ions were observed to dominate the mass spectrum. In that study, the relative amount of  $\text{D}^+$  increases with increasing coverage. For irradiation of  $\text{H}_2\text{O}$  ice with pulses of 38 eV photons  $\text{H}_3\text{O}^+$  ions are observed, but are found to be lower than  $\text{O}^+$ ,  $\text{OH}^+$  and  $\text{H}_2\text{O}^+$  ions. In the following the major ions signals of  $\text{H}^+$ ,  $\text{O}^+$ , and  $\text{O}_2^+$  from the measurements of the  $\text{H}_2\text{O}$  ice surface are analysed in more detail.

Figure 3 shows the velocity distribution of  $\text{H}^+$ ,  $\text{O}^+$ , and  $\text{O}_2^+$  ion products observed after applying FEL pulses at a

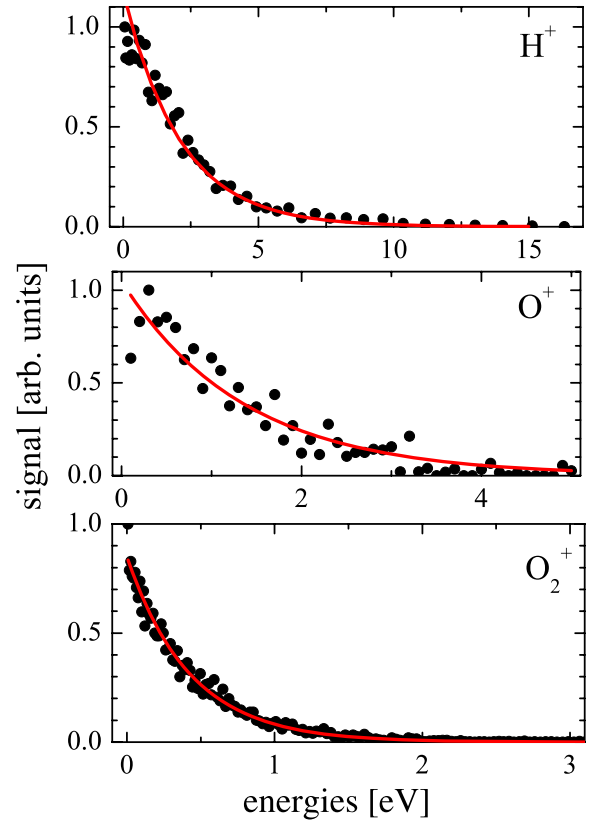


**Figure 4.** Energy distribution of the desorbing ions with a exponential fit which yields kinetic energies of 2.1 eV, 1.4 eV and 428 meV for  $\text{H}^+$ ,  $\text{O}^+$  and  $\text{O}_2^+$  ions, respectively.

38 eV photon energy. Fast and energetic reaction products are observed. To estimate the energy release Maxwellian flux distributions are fitted to the data. For  $\text{H}^+$  ions two distributions with kinetic temperatures of 7000 and 19000 K are required to fit the data with relative yields of 45% and 55%. The photon energies applied are sufficiently high to cause excitation out of both the  $1b_1$  and  $3a_1$  orbitals. The bimodality of the kinetic energy distribution observed here thus supports conclusions about its microscopic origin, by Orlando and co-workers, obtained from electron stimulated desorption [20–23]. Similarly, for  $\text{O}^+$  a kinetic temperature of about 6500 K is found, while for  $\text{O}_2^+$  two distributions with 1700 and 4500 K and respective relative intensities of 53% and 47% are again observed. This yields average energies of 1.8 eV, 840 meV and 390 meV for  $\text{H}^+$ ,  $\text{O}^+$  and  $\text{O}_2^+$  ions, respectively. It should be kept in mind that for a flux distribution the average kinetic energy  $\langle E_{\text{kin}} \rangle$  is given by  $2 kT$ .

A different understanding may be obtained from the kinetic energy distributions, as shown in figure 4 for the three ions. Fitting these distributions with an expression often used in plasma physics to obtain kinetic temperatures,

$$W(E_{\text{kin}}) \simeq \alpha \frac{1}{\sqrt{T}} \exp\{-E_{\text{kin}}/kT\}, \quad (1)$$

the conditions of the adsorbate layers pumped by the XUV pulse during the emission of the ions may be assessed. Here we obtain temperatures of 16 245 K (2.1 eV), 10 550 K (1.4 eV)

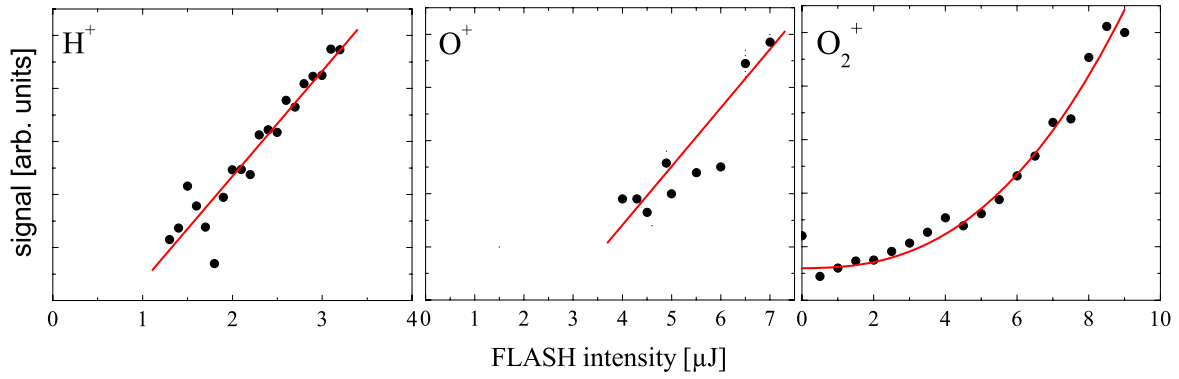


**Figure 5.** Desorption yield of  $\text{H}^+$  and  $\text{O}^+$  at 38 eV with a  $\text{H}_2\text{O}$  covered surface. The presented data for the  $\text{O}_2^+$  desorption yield were measured for a  $\text{D}_2\text{O}$  covered surface and with a photon energy of 58 eV. Similar measurements on  $\text{H}_2\text{O}$  ice and energies of 38 eV also show a nonlinear yield with  $n \sim 3$ , but occasionally even up to  $n \sim 10$ .

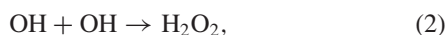
and 3311 K (428 meV) for  $\text{H}^+$ ,  $\text{O}^+$  and  $\text{O}_2^+$  ions, respectively. These rather global considerations may serve as a starting point for a more detailed understanding obtained, e.g., by molecular dynamics simulations.

The XUV radiation at 38 eV is completely absorbed in even the thinnest molecular ice layers prepared in this study. In a simple picture the dissociative process may then be initiated in a single water molecule. If one assumes a single bond cleavage of  $\text{H}_2\text{O}$  for the production of  $\text{H}^+$  ions with  $h\nu = 38$  eV radiation, a maximum excess energy of  $E_{\text{exc}} = 19.24$  eV is available. Obviously the number of  $\text{H}^+$  ions with energies close to this value is negligibly small. The majority show energies of  $E_{\text{kin}} = 2$  eV or less. Therefore most of the energy is lost in collisions and reactions with neighbouring constituents in the molecular ice. Similar energetic considerations for  $\text{O}^+$  and  $\text{O}_2^+$  ions lead to possible excess energies of  $E_{\text{exc}} = 14.83$  eV and 11.99 eV, respectively. It is obvious that in neither case are these possible kinetic energies reached. Therefore a reaction cascade has to be invoked to account for the observed kinetic energies. It is therefore obvious that the ions observed originate from the bulk ice excited by the XUV radiation. Ionic dissociation of the top most layer contributes only a negligible signal. A full understanding of the dynamic processes will also require information about the neutral desorbed species, unfortunately not available in the present study.

### 3.2. Fluence dependence

For all three ions the desorption yield is measured as a function of XUV laser fluence, see figure 5. For  $\text{H}^+$  and  $\text{O}^+$  ions a linear fluence dependence is found, while for  $\text{O}_2^+$  a highly nonlinear dependence of the yield  $Y$  on the fluence  $F$ ,  $Y = F^n$ , with an exponent of  $n = 2.5$  is observed. This varies for different runs in the range of  $n = 2$ –3, and occasionally even up to  $n = 10$ .

The linear fluence dependence of the  $\text{H}^+$  and  $\text{O}^+$  yields points toward a desorption induced by a direct electronic transition within the adsorbate to a repulsive potential curve. The formation of  $\text{O}_2^+$  requires a reaction chain involving two hydroxyl radicals to form  $\text{H}_2\text{O}_2$



and the subsequent sequential or simultaneous loss of the hydrogen atoms. These reactions have been identified as occurring in electron stimulated desorption at similar electron energies [24]. The nonlinear yield dependence suggests that the provision of a high density of energetic photons or electrons during the 30 fs XUV pulse favourably supports this reaction. At present it must remain unsolved at which step multiple electronic transitions might support the reaction. The integration of a two-pulse correlator for XUV radiation [25] into the FLASH beamlines in the up-coming shut-down will enable studies which might identify a pure electronic origin or additional vibrational contributions to this nonlinear yield dependence.

## 4. Conclusion

We have studied photochemical effects on ice surfaces with XUV pulses from FLASH. The first nonlinear reaction dynamics at surfaces with photons in the soft x-ray regime are reported. For desorbing fragment ions, velocity and energy distributions are measured, yielding energies which account for only a small part of the available excess energy. The ions observed thus originate from the excited bulk ice. The observation of a nonlinear behaviour for the  $\text{O}_2^+$  yield calls for a two-pulse correlated desorption experiment in order to yield more insight into the microscopic processes. This kind of measurement can be performed with an autocorrelator specified for use in the soft x-ray regime with a temporal resolution of better than a femtosecond [25].

## Acknowledgments

The authors thank the FLASH-Team at HASYLAB and acknowledge partial financial support by the Bundesministerium für Bildung und Forschung via grant No. 05 KS4PMC/8.

## References

- [1] Stockbauer R, Hanson D M, Flodström S A and Madey T E 1982 *Phys. Rev. B* **26** 1885
- [2] Kurtz R L, Stockbauer R, Madey T E, Román E and de Segovia E R 1989 *Surf. Sci.* **218** 178

- [3] Rosenberg R A, Rehn V, Jones V O, Green A K, Parks C C, Loubriel G and Stulen R H 1981 *Chem. Phys. Lett.* **80** 488
- [4] Chakarov D V, Österlund L and Kasemo B 1995 *Langmuir* **11** 1201
- [5] Chakarov D and Kasemo B 1998 *Phys. Rev. Lett.* **81** 5181
- [6] Chakarov D V, Gleeson M A and Kasemo B 2001 *J. Chem. Phys.* **115** 9477
- [7] Westley M S, Baragiola R A, Johnson R E and Baratta G A 1995 *Nature* **373** 405
- [8] Westley M S, Baragiola R A, Johnson R E and Baratta G A 1995 *Planet. Space Sci.* **43** 1311
- [9] Gerakines P A, Schutte W A and Ehrenfreund P 1996 *Astron. Astrophys.* **312** 289
- [10] Watanabe N, Horii T and Kouchi A 2000 *Astrophys. J.* **541** 772
- [11] Öberg K I, Linnartz H, Visser R and van Dishoeck E F 2009 *Astrophys. J.* **693** 1209
- [12] Baggott S R, Kolasinski K W, Perdigao L M A, Riedel D, Guo Q and Palmer R E 2002 *J. Chem. Phys.* **117** 6667
- [13] Mitzner R, Sorokin A A, Siemer B, Roling S, Rutkowski M, Zacharias H, Neeb M, Noll T, Siewert F, Eberhardt W, Richter M, Juranic P, Tiedtke K and Feldhaus J 2009 *Phys. Rev. A* **80** 025402
- [14] Chakarov D V, Österlund L and Kasemo B 1995 *Vacuum* **46** 1109
- [15] Gross E, Horowitz Y and Asscher M 2005 *Langmuir* **21** 8892
- [16] Smith R S, Huang C, Wong E K L and Kay B D 1996 *Surf. Sci.* **367** 240
- [17] Speedy R J, Debenedetti P G, Smith R S, Huang C and Kay B D 1996 *J. Chem. Phys.* **105** 240
- [18] Henke B L, Gullikson E M and Davis E M 1993 *Atomic Data Nucl. Data Tables* **54** 181
- [19] Hubbell J H, Veigele W J, Briggs E A, Brown R T, Cromer D T and Howerton R J 1975 *J. Phys. Chem. Ref. Data* **4** 471
- [20] Kimmel G A, Orlando T M, Cloutier P and Sanche L 1997 *J. Phys. Chem. B* **101** 6301
- [21] Kimmel G A and Orlando T M 1996 *Phys. Rev. Lett.* **77** 3983
- [22] Kimmel G A and Orlando T M 1996 *Phys. Rev. Lett.* **75** 2606
- [23] Simpson W C, Orlando T M, Parenteau L, Nagesha K and Sanche L 1998 *J. Chem. Phys.* **108** 5027
- [24] Johnson R E, Cooper P D, Quickenden T I, Grieves G A and Orlando T M 2005 *J. Phys. Chem.* **123** 184715
- [25] Mitzner R, Siemer B, Neeb M, Noll T, Siewert F, Roling S, Rutkowski M, Sorokin A A, Richter M, Juranic P, Tiedtke K, Feldhaus J, Eberhardt W and Zacharias H 2008 *Opt. Express* **16** 19909